IFSCC 2025 full paper (IFSCC2025-1551)

"Addressing Rheology and Performance Challenges in Non-Sulfate Formulations with Functional Polysaccharides"

Janet R. McMillan [1*], Ann C. Fernandez[1], Wenzhao Yang[1], Bryan Caruso[1], Michaeleen Pacholski[1], Shashank Kamdar[1], John Riley[1], Shannon Golden[1], Stephanie Hughes[1], Anthony Roehr[1]l, Anirudha Banerjee[2], Hammad Faizi[2], Lyndsay Leal[2], Daniel Almeida[2], Hélène Dihang[2]

[1] Core Research & Development, The Dow Chemical Company. [2] Dow Consumer Solutions, The Dow Chemical Company.

*E-mail: jmcmcillan3@dow.com

1. Introduction

Consumer trends in the rinse-off personal care space towards "sulfate-free" product formats are rapidly rising; what was once a niche product offering, today represents close to half of global new shampoo product launches **[1]**. Many alternative non-sulfate surfactants have larger head group areas and higher curvature as compared to their sulfate counterparts, which introduce a range of formulation challenges spanning worm-like micelle formation and rheology, foaming and conditioning performance **[2]**. In addition, there is growing pressure to replace synthetic non-biodegradable thickening polymers such as acrylates. Thus, reformulation to achieve desired performance along with improved sustainability profiles, traditional formulation paradigms need to be re-imagined **[3]**.

Cellulose ethers are a class of bio-based functional polymers that are used ubiquitously in personal care formulations and are attractive due to their multi-functional performance benefits, spanning deposition, foam boosting and rheology modification. The solution phase behavior of non-ionic cellulose ethers with surfactants has been widely explored with sulfated and alkoxylate surfactants, where polymer functionality, hydrophobic substitution, and molecular weight, in addition to surfactant charge and aggregation number are all important considerations in controlling phase behavior and rheology **[4–8]**. However, the behavior of cellulose ethers with non-sulfate surfactants has remained largely unexplored. Therefore, as formulators seek to reformulate away from conventional laureth-sulfate surfactants, there is an emerging need to explore the phase behavior, rheology and other performance benefits of cellulose ethers in non-sulfate systems.

The following work establishes the utility of functional polysaccharides, specifically hydroxypropylmethyl cellulose (HPMC) and dual cationically modified dextran (Dual catDex), at addressing foaming, rheology, and deposition performance challenges in non-sulfate systems. We focus initially on understanding polymer entanglement regimes and phase behavior in the

presence of surfactants using high-throughput formulation, phase characterization and viscosity screening capabilities, demonstrating the high compatibility of HPMC with non-sulfate surfactants and underscoring important stability advantages of propoxylation over hydroxyethyl modifications. Next, we investigate the shear and extensional rheology of model shampoos thickened with HPMC, demonstrating the similarity in the texture compared with benchmark shampoos, and report low (<10 s) filament breakup times, indicating the absence of any stringy texture. Finally, foaming and silicone deposition are studied in a model conditioning shampoo in combination with cationic dextran, where an unexpected benefit of increasing silicone deposition at increasing HPMC use levels is reported, along with the high flash foam and slow liquid drainage of HPMC/Dual catDex shampoo over benchmarks. Overall, this work provides a novel approach and formulation guide to resolve viscosity, deposition and foaming challenges in non-sulfate formulations leveraging the multi-faceted benefits of functional polysaccharides.

2. Materials and Methods

2.1 Materials: Table 1 lists formulation ingredients used in this work and corresponding abbreviations used in figure captions throughout the text.

Table 1. Ingredient list of raw materials used in this study.

Ingredient INCI	Ingredient Role	Ingredient Abbreviation
Hydroxypropyl Methylcellulose	Rheology modifier	HPMC
Hydroxyethylcellulose	Rheology modifier	HEC
Amodimethicone (and) C11-15 Alketh-12 (and) C11-15 Alketh-7	Silicone conditioning emulsion	Si Emulsion
Polyquaternium-10	Deposition polymer	Cat-HEC
Dextran Hydroxypropyltrimonium/Laurdimonium Chloride	Deposition polymer	Dual catDex
Cocamidopropyl betaine	Amphoteric surfactant	CapB
Alpha olefin sulfonate	Anionic surfactant	AOS
Sodium cocoyl isethionate	Anionic surfactant	SCI
Decyl glucoside	Non-ionic surfactant	APG
Sodium lauryl sarcosinate	Anionic surfactant	SL Sarcosinate
Sodium cocoyl glutamate	Anionic surfactant	SC Glutamate

2.2. HTR workflow to prepare and characterize shampoos: A highthroughput (HTR) workflow was utlized for formulation preparation and characterization related to polymer phase behavior screening. The general workflow is shown in Scheme 1 and the different steps of the HTR workflow are described in detail below.

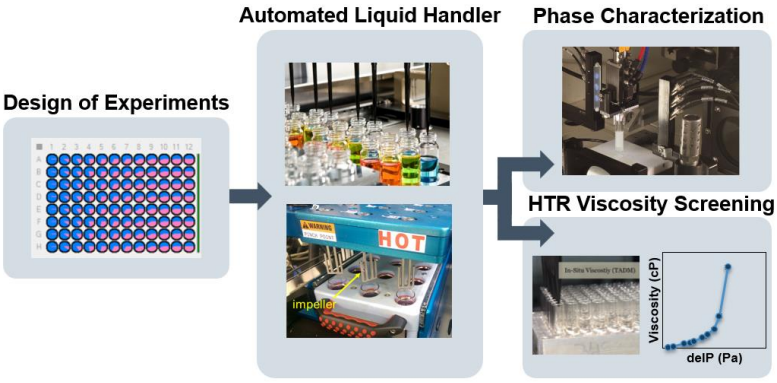

Scheme 1. HTR workflow for shampoo preparation and characterization. After the formulations were designed, an automated liquid handler was used to dispense liquids. After preparation, shampoos were characterized using a custom automated vial imaging and viscosity screening tools described below.

2.2.1 Formulation design and preparation: All experiments were designed using a Library Studio software. Samples were prepared by first pre-hydrating non-ionic cellulose ethers in 2 wt% solutions in MilliQ water using an overhead mixing setup on a 50-100 g scale. A Hamilton MicroStar liquid handler equipped with a custom overhead stirring and mixing deck was used for subsequent formulating. First, water, deposition aid polymer, and pre-hydrated non-ionic HEC were added and mixed for 20 min at 300 rpm. Subsequently, surfactants were added while heating to 60 °C and continuously mixing. After the formulations were allowed to cool to room temperature, 10 wt% citric acid was used to adjust the pH to 6.0-6.7, followed by the addition of the silicone emulsion where applicable. Model formulation compositions used in this work are provided in Tables 2 and 3.

Table 2. General composition for model formulation 1. The surfactant mixtures are comprised of a fixed total surfactant use level of 15 wt% actives, where the first entry provided indicates use levels for formulations that do not contain APG. For ingredient classes where multiple types are investigated, they are listed sequentially in the same entry. The balance of the formula is water.

Ingredient INCI(s)	Ingredient Role	Use level range [wt%]
Hydroxypropyl Methylcellulose, Hydroxyethylcellulose	Rheology modifier	0-1.2
Polyquaternium-10	Deposition polymer	0.3
Cocamidopropyl betaine	Amphoteric surfactant	3.8, 2.6
Sodium lauryl sarcosinate	Anionic surfactant 1	7.5, 5.3
Alpha olefin sulfonate, Sodium cocoyl isethionate	Anionic surfactant 2	3.4, 2.6
Decyl glucoside	Non-ionic surfactant	0, 4.5

Table 3. General composition for model conditioning formulation 2.

Ingredient INCI(s)	Ingredient Role	Use level range [wt%]
Hydroxypropyl Methylcellulose	*Rheology modifier*	0.5-1.6

Dextran Hydroxypropyltrimonium/Laurdimonium Chloride	Deposition polymer	0.3
Amodimethicone (and) C11-15 Alketh-12 (and) C11-15 Alketh-7	Silicone conditioning emulsion	0.5-1.0
Cocamidopropyl betaine	Amphoteric surfactant	4.5
Sodium cocoyl glutamate	Anionic surfactant 1	6.3
Sodium cocoyl isethionate	Anionic surfactant 2	2.7
Decyl glucoside	Non-ionic surfactant	4.5

2.2.2 HTR Method for Viscosity Screening: HTR viscosity screening measurements were done on a Hamilton Microlab Star using a Total Aspiration Dispense Monitoring (TADM) as described previously [9]. A custom calibration method was set up using 10 kinematic viscosity standards with viscosities ranging from 103 to 12640 cP. High volume tips with a diameter of 0.7 mm were used and the aspiration/dispense volumes were set to 50 µL at a flow rate of 5 µL/s. The viscosities of the standards were plotted against the corresponding changes in pressure (delP) to obtain a calibration curve. For viscosity analyses, test material delP values were first obtained on TADM and the calibration curve was used to calculate test material viscosities at a shear rate of approximately 148 s^{-1} via linear interpolations between calibration standards.

2.2.3 HTR Method for Imaging: Formulations were imaged using a robot built in-house called the Phase Identification and Characterization Apparatus (PICA) **[10,11]**. For general imaging, samples were illuminated with a LED light source held at a 90° angle relative to a high-resolution camera.

2.3 Low concentration polymer viscosity measurements: To estimate the apparent critical overlap concentration of HPMC and HEC, polymer solutions varying in concentration between 1 to 10,000 ppm were prepared in a 96-well plate using a MicroStar Hamilton liquid handler. The HTR screening method described above was used to measure viscosities of the samples, with the modification of flow rate to 100 µL/s. Apparent c* values were determined by plotting HTR viscosity as a function of HPMC level by identifying the inflection point in the plot. The c* values are being referred to here are apparent c* since viscosities estimation method approximates to a shear rate of 3000 s^{-1}.

2.4 Shear and Extensional Rheology: Shear rheology characterization was performed on a TA Instruments DHR-3 Hybrid Rheometer equipped with an upper 40 mm 2° stainless steel cone and plate fixture with a lower Peltier plate for temperature control. All tests were performed at 22 °C and follow the procedure below:

1. Peak hold at 10 1/s for 90 seconds ; used to measure a steady shear viscosity that is comparable to a Brookfield-spindle viscosity
2. Frequency sweep at 2% strain from 100 rad/s down to 0.1 rad/s; used to measure the linear-viscoelastic properties and identify a cross-over frequency associated with worm-like micelle network dynamics.
3. Repeat peak hold from step 1 to recondition the sample
4. Flow sweep from 0.01 1/s up to 1000 1/s ; used to characterize the shear thinning flow behavior.

A Haake CaBER 1 extensional rheometer was used for extensional testing of shampoos[12]. Samples are loaded onto 6 mm stainless steel plates at an initial gap size of 3 mm using a positive displacement pipette to form a liquid bridge between the two plates. The plates are then separated from an initial height of 3 mm to a final height of 10 mm using a fast, linear strike profile over 75 ms. All tests are made at ambient temperature, and each sample was tested in duplicate with a fresh loading. Filament stretching profiles (filament diameter vs time) are analyzed for the overall filament breakup time and elastocapillary relaxation time.

2.5 Hair treatment: Hair tresses used in this study are 4 h bleached medium brown hair provided by International Hair Importers & Products, USA. Tresses were 15 cm in length and 1 g each. Prior to applying the formulation, each tress was pre-washed under running tap water for 30 s. Excess water was removed by squeezing tresses with two fingers, followed by the application of 0.2 g of 9% Sodium Lauryl Sulfate (SLS) solution per gram of hair. After the tresses were massaged gently with fingers for 30 s, they were rinsed under running tap water for 1 min to remove the SLS. Excess water was removed again by squeezing the tresses with two fingers. Test shampoos were applied at 0.4 g of material per gram of hair. The tresses were massaged for 1 min and then rinsed for 30 s and finally left to air dry overnight in a controlled room at 50% humidity.

2.6 X-ray Photoelectron Spectroscopy (XPS): To quantitate silicone deposition on hair, samples were analyzed as received by taping sections of hair tresses to double-sided tape. Data were taken from regions where no underlying tape was optically visible. X-ray photoelectron spectroscopy (XPS) gives quantitative elemental and chemical state information from the top 10 nm. XPS data were acquired from four areas across 1 cm × 3 mm from the center of the tress.

2.7 Foam Analysis: Foam analysis of samples was conducted using a Kruss Dynamic Foam Analyzer – DFA100. Formulations were diluted to 6 wt% using MilliQ water immediately prior to measurement and stirring gently for 2 min using a magnetic stir bar to combine. 50 mL of the diluted solution was then added to the instrument and mixed at 4000 rpm for 10 s with a 5 s oscillation time. Post agitation, data was collected for 5 min.

2.8 Predictive model fitting: Models were fit to experimental foaming, HTR viscosity and silicone deposition data on formulations presented in Table 2 using JMP Pro 18 software using a standards least squared response surface model, with pruned forward selection methods used to control overfitting. R^2 values for all model predictions shown fall between 0.69-0.95.

3. Results and Discussion

3.1 Cellulose ether dilute viscosity and phase behavior with surfactants

To understand the utility HPMC and HEC in non-sulfate applications, we began by exploring polymer entanglement and phase behavior of these materials with surfactants mixtures of interest. First, polymer critical entanglement concentration regimes (c*) were probed via HTR methods to map polymer solution viscosity as a function of polymer concentration as shown in Figure 1. For HPMC containing solutions, it was observed that viscosities were consistent up a certain value and beyond this concentration, there was a sharp rise in solution viscosity. HPMC apparent c* value was estimated to be 1500 ppm and this concentration represents the border between dilute and semi-dilute regimes. However, HEC behaved differently in comparison to HPMC and the estimation of an apparent c* value was not possible over the concentration range probed.

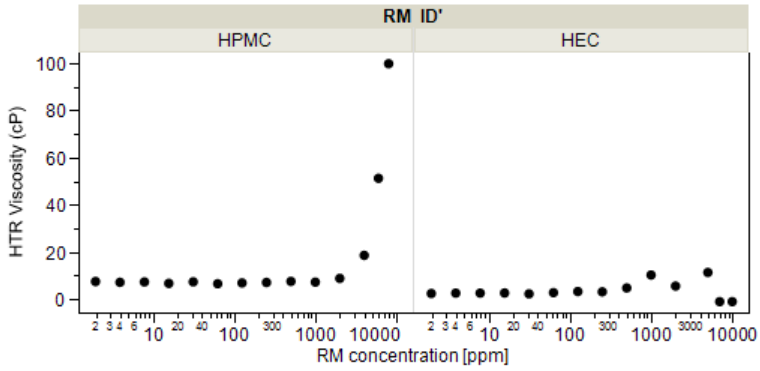

Figure 1. Viscosity vs polymer concentration trends under dilute conditions for HPMC and HEC polymers. The apparent c* value for HPMC was estimated by plotting the viscosities of the polymers as a function of polymer concentration to understand the transition from dilute to semi-dilute regions for the polymer.

Next, phase behavior and stability were studied for formulations containing HPMC and HEC in the presence of surfactants, with mixtures detailed in Table 1. Figure 2A shows the relative solution clarity of these polymers in combination with different anionic surfactant packages in the presence and absence of APG. All formulations incorporating HPMC had high clarity and were single phase (Figure 2B). In contrast, HEC formulations were turbid at higher polymer levels (Figure 2A) and produced 2-phase formulations as shown in Figures 2B and 2C.

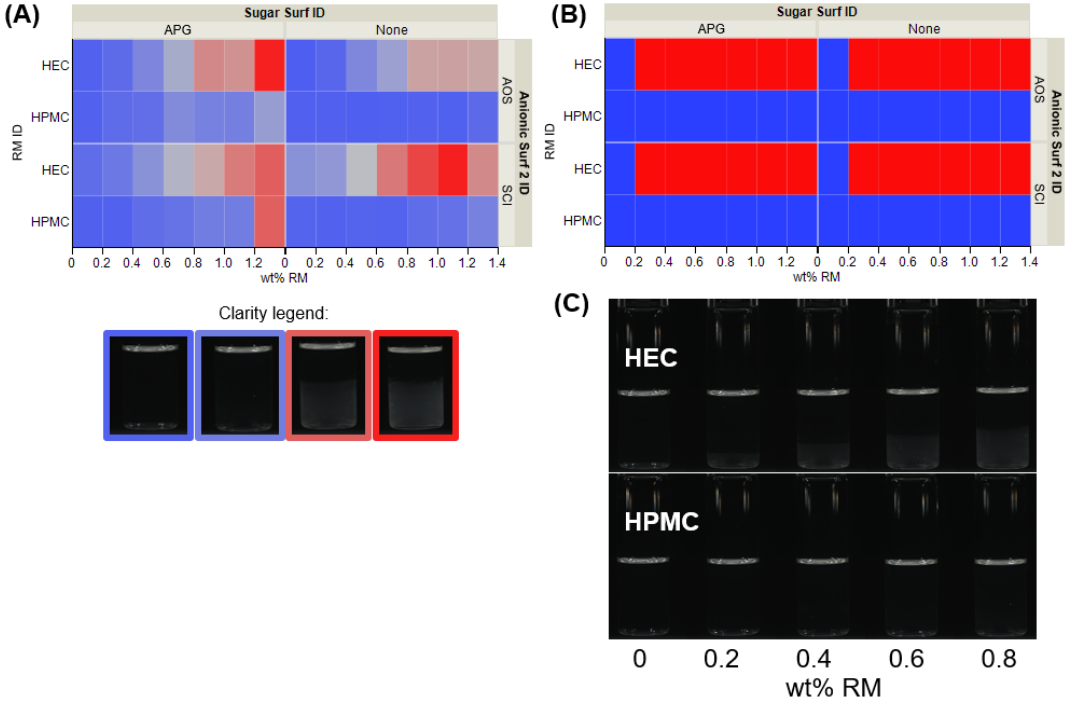

Figure 2. Phase behavior of HPMC and HEC containing shampoos. A) Shampoo clarity; B) Number of phases in shampoo where blue is 1 phase and red is 2 phases; C) Images of HEC and HPMC shampoos.

3.2 Rheology of HPMC-thickened shampoos

Having demonstrated the robust phase stability of HPMCs with non-sulfate surfactants, we next turned to understanding the resulting textures and feel achieved with HPMC-containing

shampoos. A subset of the formulations assessed above were evaluated via conventional shear and extensional rheology techniques against a series of commercial shampoos. Shear rheology is critical to assessing the flowability and spreadability of the product as it is applied by the consumer, and extensional rheology can provide insight into response of the fluid under extensional flow, where high filament breakup times may indicate consumer-perceivable stringiness **[13]**. Figure 3 summarizes this shear (A) and extensional (B) rheological evaluation of the experiment solutions. The flow curves of these formulations are remarkably similar to commercial shampoos, showing a characteristic shear-thinning profile that is desirable for the application. In oscillatory experiments, we observe a cross-over frequency in the range of 8-70 rad/s, a similar magnitude to the range of 40-100 rad/s measured for benchmarks.

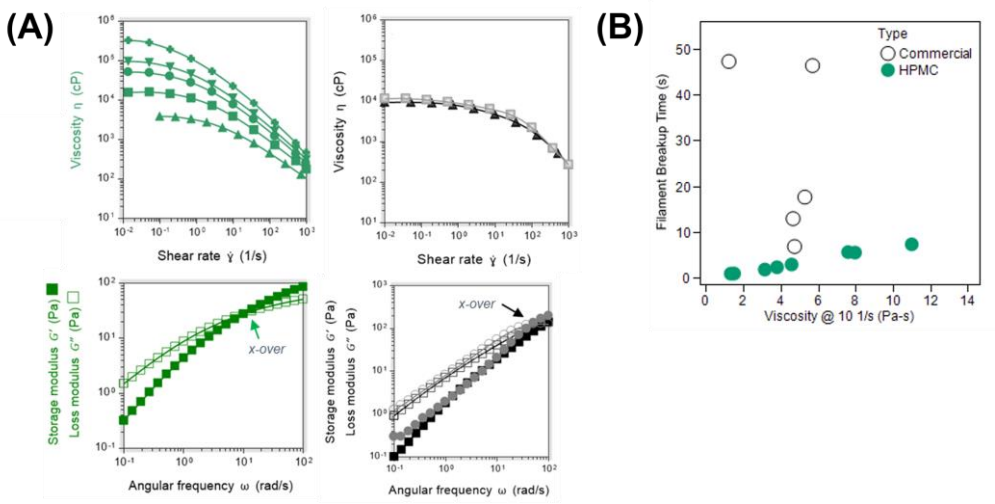

Figure 3. Rheological properties of HPMC-containing shampoos. (A) Shear rheology showing (top) and (bottom) of HPMC-containing shampoos (green, left) and commercial benchmarks (grey, right). (B) Filament breakup times measured via CaBER plotted against shear viscosity at 10 s^{-1}.

The filament breakup times summarized in Figure 3B show increasing filament breakup time with increasing shear viscosity as the HPMC concentration is increased. Importantly, the filament breakup times observed for the model formulations fall below all commercial benchmarks assessed, even at equivalent shear viscosity. Overall, this rheological assessment supports that shampoo-like textures can be achieved in non-sulfate systems where HPMC is used as a primary thickening ingredient.

3.3 Performance modelling of HPMC-thickened conditioning shampoos

To develop further the understanding of the interactions and performance of HPMCs in non-sulfate containing formulations to achieve a holistic balance of viscosity, foaming and silicone deposition, experiments were designed according to Table 3. These experiments assessed the impact of HPMC use level and silicone emulsion use level on overall performance, where foaming, viscosity and deposition were investigated simultaneously. Figure 4 presents a summary of key findings from the foaming behavior of the experimental shampoos, where it is seen that the HPMC-containing shampoos result in higher foam height as the HPMC level is increased, which exceeds that of commercial benchmarks evaluated. We also investigated the rate of liquid drainage, which shows that the increase in liquid height, and thus foam drainage, slows considerably as HPMC use level is increased, demonstrating not only improved flash foam, but also improved stability of benchmark shampoos.

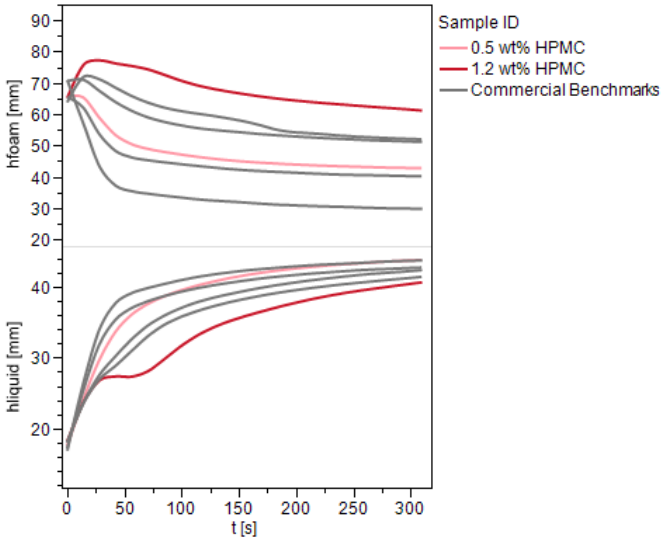

Figure 4. Foaming performance of HPMC-containing conditioning formulations. Top: foam height data vs time for formulations containing 1 wt% Si plotted against select commercial shampoos diluted at equivalent dilution; bottom: Foam drainage trends between HPMC-containing and commercial formulations showing the measured liquid height in mm over time after foam generation.

To understand formulation performance holistically beyond foaming, Figure 5 shows the resulting model predictions plotted as performance heat maps against the HPMC and silicone use levels, where initial foam height at t=30 s is used for modelling. We observe that increasing the HPMC use level beyond 0.8 wt% in the formulation results in foam height close to 80 mm, which exceeds all commercial benchmarks tested in this study, and silicone use level has minimal impact on foaming performance. Importantly, the model predictions demonstrate an expected trend of increasing silicone deposition as emulsion usage is increased. Surprisingly, we find that increasing the HPMC use level also results in improved silicone deposition, where the region of high silicone deposition performance is extended to 0.65 wt% emulsion level. Finally, we find that viscosity is driven entirely by HPMC use level, where shampoo-like viscosities can be obtained at or above 1.2 wt% of HPMC.

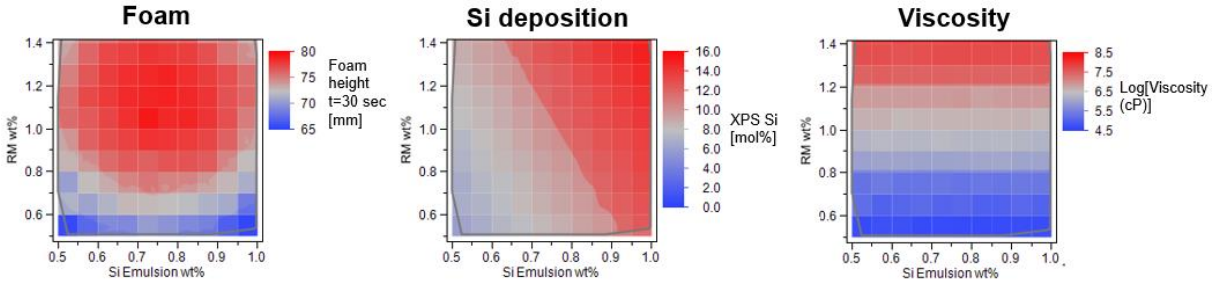

Figure 5. Model prediction results for foam, silicone deposition and viscosity in HPMC-containing conditioning shampoos.

5. Discussion

The differences in entanglement regimes and phase behavior between HPMC and HEC can be explained by the presence (or absence) of hydrophobes on the polymers. HPMC contains hydroxypropyl and methyl hydrophobic units that can drive polymer association and entanglement in solution at lower concentrations than HEC, which is overall more water soluble and does not self-associate over the concentration range probed. With the resulting change in slope and rise in solution viscosity with increasing HPMC concentration, as seen in Figure 1, the apparent c* value can be estimated. In addition to this, the high clarity and phase stability of HPMC shampoos (Figure 2) with a broad range of surfactant combinations tested can also be explained due to favorable interactions between the polymer hydrophobes and surfactant micelles, resulting in a crosslinked network. This is in agreement with past work on alkoxylate and sulfate surfactants **[6,14]**. On the other hand, the lack of hydrophobic character of HEC does not favor such associative behavior, resulting in an entanglement regime above the concentration range probed. This would also mean that favorable surfactant-polymer interactions are not possible in the HEC system, resulting in turbid and phase destabilized HEC shampoos due to entropic depletion effects (Figure 2) **[14]**.Thus, HPMCs present an advantage as compared with HECs in their compatibility in high-surfactant applications such as non-sulfate shampoos. The rheological characterization of HPMC-containing surfactant formulations showing shear-thinning behavior is consistent with previous reports **[15]**. The extensional behavior demonstrate that non-stringy textures are easily achievable in HPMC-thickened formulations, despite the hypothesized presence of polymer-surfactant complexes. Importantly, these results establish that HPMCs are compatible and effective at network building with non-sulfate surfactants that are difficult to thicken via conventional worm-like micelle mechanisms.

Investigating other aspects of performance in a model conditioning shampoo, several expected findings were established, including the impact of HPMC concentration on increasing flash foam height and slowing liquid draining, as well as the dependence of the viscosity on HPMC concentration **[16]** . A key unexpected finding uncovered in this performance investigation is the sensitivity of silicone deposition to HPMC use level, where increasing the polymer level can enable high deposition over a broader range of emulsion concentrations when used in combination with a dual cationically modified dextran. Taken together, these results indicate that shampoo performance can be optimized by increasing HPMC use level to 1.2 -1.4 wt% to both achieve a shampoo-like viscosity, while improving foam. At this use level, high silicone deposition performance can be maintained while the emulsion level is reduced to 0.6 wt%. These findings further suggest a benefit of using HPMC to as a thickening solution while achieving improved foaming and deposition.

5. Conclusion

In conclusion, we have investigated polymer entanglement, non-sulfate surfactant phase behavior, rheology, and holistic performance of shampoos containing HPMC as a primary thickening polymer. Our findings highlight the advantage of this class of cellulose ethers at driving surfactant compatibility over HEC, and we establish that shampoo-like textures can be achieved when HPMCs are used with difficult-to-thicken non-sulfate surfactants. Beyond compatibility and rheology, we have demonstrated the HPMCs can be used in combination with cationic dextran deposition polymers to achieve robust foaming, and high silicone deposition performance, where increasing HPMC leads to unexpected improvements in deposition onto damaged hair at low silicone dosages. Together, this combination of functional polysaccharides enables the design of next generation high-performing non-sulfate formulations with sustainable raw materials.

6. References

1. Mintel GNPD Database Available online: https://www.mintel.com/products/gnpd/.

2. Su, E.; Herman, S. Beyond Sulfate-Free Personal Cleansing Technology. *Cosmetics* **2025**, *12*, 14, doi:10.3390/cosmetics12010014.
3. Luengo, G.S.; Leonforte, F.; Greaves, A.; Rubio, R.G.; Guzman, E. Physico-Chemical Challenges on the Self-Assembly of Natural and Bio-Based Ingredients on Hair Surfaces: Towards Sustainable Haircare Formulations. *Green Chem.* **2023**, *25*, 7863–7882, doi:10.1039/d3gc02763e.
4. Thuresson, K.; Söderman, O.; Hansson, P.; Wang, G. Binding of SDS to Ethyl(Hydroxyethyl)Cellulose. Effect of Hydrophobic Modification of the Polymer. *J. Phys. Chem.* **1996**, *100*, 4909–4918, doi:10.1021/jp9520411.
5. Nilsson, S. Interactions between Water-Soluble Cellulose Derivatives and Surfactants. 1. The HPMC/SDS/Water System. *Macromolecules* **1995**, *28*, 7837–7844, doi:10.1021/ma00127a034.
6. Drummond, C.J.; Albers, S.; Furlong, D.N. Polymer—Surfactant Interactions: (Hydroxypropyl)Cellulose with Ionic and Ion-Ionic Surfactants. *Colloids Surf.* **1992**, *62*, 75–85, doi:10.1016/0166-6622(92)80038-4.
7. Joshi, S.C.; Chen, B. Influence of Surfactant Properties on Thermal Behavior and Sol–Gel Transitions in Surfactant-HPMC Mixtures. *J. Appl. Polym. Sci.* **2009**, *113*, 2887–2893, doi:10.1002/app.30317.
8. Silva, S.M.C.; Antunes, F.E.; Sousa, J.J.S.; Valente, A.J.M.; Pais, A.A.C.C. New Insights on the Interaction between Hydroxypropylmethyl Cellulose and Sodium Dodecyl Sulfate. *Carbohydr. Polym.* **2011**, *86*, 35–44, doi:10.1016/j.carbpol.2011.03.053.
9. Deshmukh, S.; Bishop, M.T.; Dermody, D.; Dietsche, L.; Kuo, T.-C.; Mushrush, M.; Harris, K.; Zieman, J.; Morabito, P.; Orvosh, B. A Novel High-Throughput Viscometer. *ACS Combinatorial Science* **2016**, *18*, 405–414.
10. Bilodeau, C.; Jin, W.; Xu, H.; Emerson, J.A.; Mukhopadhyay, S.; Kalantar, T.H.; Jaakkola, T.; Barzilay, R.; Jensen, K.F. Generating Molecules with Optimized Aqueous Solubility Using Iterative Graph Translation. *React. Chem. Eng.* **2021**, *7*, 297–309, doi:10.1039/d1re00315a.
11. McMillan, J.R.; Miller, D.S.; Nimako-Boateng, C.; Wilson, L.; Kuo, T.; Tesoldi, M.F.; Young, T.; Izmitli, A. The Interfacial Properties of Biosurfactant Mixtures. *J. Surfactants Deterg.* **2024**, doi:10.1002/jsde.12777.
12. Nakatani, A.I. (A) *CaBER Analysis of HmHEC Solutions and Shampoos*; 2020;
13. Davies, A.; Amin, S. Rheology of Cosmetic Products: Surfactant Mesophases, Foams and Emulsions. *J. Cosmet. Sci.* **2020**, *71*, 481–496.
14. Robb, I.D.; Williams, P.A.; Warren, P.; Tanaka, R. Phase Separation in Concentrated Mixtures of Polymers and Surfactants. *J. Chem. Soc., Faraday Trans.* **1995**, *91*, 3901–3906, doi:10.1039/ft9959103901.
15. Katona, J.M.; Njaradi, S.Đ.; Sovilj, V.J.; Petrović, L.B.; Marčeta, B.B.; Milanović, J.L. Rheological Properties of Hydroxypropylmethyl Cellulose/Sodium Dodecylsulfate Mixtures. *J. Serbian Chem. Soc.* **2014**, *79*, 457–468, doi:10.2298/jsc130807132k.
16. Perticaroli, S.; Herzberger, J.; Sun, Y.; Nickels, J.D.; Murphy, R.P.; Weigandt, K.; Ray, P.J. Multiscale Microstructure, Composition, and Stability of Surfactant/Polymer Foams. *Langmuir : ACS J. Surf. colloids* **2020**, *36*, 14763–14771, doi:10.1021/acs.langmuir.0c02704.